*Catalysis Letters Vol. 100, Nos. 3–4, April 2005 (© 2005)*
DOI: 10.1007/s10562-004-3466-1

# $NO_2$ inhibits the catalytic reaction of NO and $O_2$ over Pt

S.S. Mulla[a], N. Chen[a], W.N. Delgass[a], W.S. Epling[a,b] and F.H. Ribeiro[a,]*

[a]*School of Chemical Engineering, Purdue University, 480 Stadium Mall Drive, West Lafayette, IN 47907-2100*
[b]*Cummins, Inc., 1900 McKinley Ave, Columbus, 47201 IN*

Received 20 October 2004; accepted 14 December 2004

The rate equation for the overall reaction of NO and $O_2$ over $Pt/Al_2O_3$ was determined to be $r = k_f[\mathrm{NO}]^{1.05\pm0.08}[\mathrm{O_2}]^{1.03\pm0.08}[\mathrm{NO_2}]^{0.92\pm0.07}(1-\beta)$, with $k_f$ as the forward rate constant, $\beta = ([\mathrm{NO_2}]/K[\mathrm{NO}][\mathrm{O_2}]^{1/2})$, and $K$ as the equilibrium constant for the overall reaction. An apparent activation energy of 82 kJ $\mathrm{mol}^{-1}$ ± 9 kJ $\mathrm{mol}^{-1}$ was observed. The inhibition by the product $NO_2$ makes it imperative to include the influence of $NO_2$ concentration in any analysis of the kinetics of this reaction. The reaction mechanism that fits our observed orders consists of the equilibrated dissociation of $NO_2$ to produce a surface mostly covered by oxygen, thereby inhibiting the equilibrium adsorption of NO, and the non-dissociative adsorption of $O_2$, which is the proposed rate determining step.

**KEY WORDS:** NO oxidation on Pt; $NO_2$ inhibition on NO oxidation; reaction orders; apparent activation energy.

## 1. Introduction

The oxidation of NO to $NO_2$ over a supported noble metal component is an important step involved in $NO_x$ abatement techniques, e.g., selective catalytic reduction (SCR) [1–3] and $NO_x$ storage/reduction (NSR) process [4] being developed for lean-burn diesel engines. These processes are a result of new regulations that limit the emissions of $NO_x$, CO and hydrocarbon (HC) from diesel engines [5]. Pt has been the oxidation catalyst of choice due to its high red–ox activity [3,6] and its presence as a major component in the current automobile exhaust (or three-way) catalysts. We studied the kinetics of this reaction over a $Pt/Al_2O_3$ catalyst and found that the forward rate is inhibited by the product $NO_2$. Previous work on the reaction kinetics of NO oxidation over Pt catalysts [1,2,7,8] did not explicitly consider the inhibitory effect of $NO_2$. This new finding is important because $NO_2$ affects the rate of reaction significantly and, thus, it needs to be included in any kinetic model for NO oxidation.

## 2. Experimental methods

The $Pt/Al_2O_3$ catalyst used in this study was supplied by EmeraChem in monolithic form. Based on a known liquid uptake of the bare monolith, the appropriate amount of $\gamma$-$Al_2O_3$ was mixed as an aqueous slurry. The bare monolith was dipped into this slurry, drained, dried and then calcined at 500 °C for 1 h. The monolith was then dipped into the Pt-containing aqueous solution such that a final Pt loading of approximately 50 $\mathrm{g/ft^3}$ of monolith was attained. The Pt was put into solution as an amine-based precursor.

The monolith had a length of 1 inch, a cross-section of 60 channels with a cell density of 200 $\mathrm{channels/in^2}$. The percentage-of metal exposed (PME) measured by $H_2$–$O_2$ titration [9] was 42%. The total sample weight was about 3 g. The conversion for the NO oxidation reaction was measured in a bench-top, plug-flow stainless steel reactor. High-temperature Zetex insulation was wrapped around the catalyst sample and placed in the reactor tube. The insulation material blocked the space between the monolith and the wall of the reactor, minimizing gas flow bypassing the catalyst. Glass beads were placed upstream of the catalyst sample to ensure mixing and uniformity of the gas flow, and the reactor was placed inside a temperature-controlled furnace. To minimize temperature gradients, the inlet gas was preheated before entering the reactor. Thermocouples were placed 6 mm before and after the catalyst sample to verify inlet and outlet gas temperatures. A reactor bypass was used to verify the nominal inlet concentrations of NO and $NO_2$. The NO and $NO_2$ concentrations in the outlet gas were continuously detected with a chemiluminescence detector (California Analytical Instruments HCLD 400). The experiments were conducted with a total flow of approximately 6.6 L $\mathrm{min}^{-1}$.

The NO-oxidation apparent activation energy and reaction orders with respect to NO, $O_2$, and $NO_2$ were measured. Before the experiments, the $Pt/Al_2O_3$ sample was pretreated at 150 °C with 10% $O_2$ in $N_2$ for 1 h followed by reduction with 0.5% $H_2$ in $N_2$ for 1.5 h with a constant total flow of approximately 6.5 L $\mathrm{min}^{-1}$. The reactor was operated in a differential manner by using an excess $NO_2$ in the feed and restricting the NO

---

* To whom correspondence should be addressed.
E-mail: fabio@purdue.edu

conversions to below 10%. During the experiments, the conversions were monitored only after flowing the feed gas for typically 1 h, to ensure that a stable conversion was obtained. At the end of each experiment, the conditions of the first data point in the series were duplicated to check for reproducibility and deactivation. For apparent activation energy tests, the temperature variation was done with a constant feed composition and constant total flow. The temperature was varied in a non-sequential manner to avoid systematic errors. Similarly, in order to determine the effect of reactant or product concentration on rate, the concentration of the species of interest was varied in non-sequential manner, while the concentrations of the other species were kept constant. The errors in the orders and activation energy were calculated through a linear least squares fit with 95% confidence intervals. The criteria suggested by Dekker *et al.* [10] were used to check external heat and mass transfer limitations. The Carberry number (Ca) and the parameter for external heat transfer limitation–given as$|(k_g(-\Delta H)C_b/hT_b)\gamma \mathrm{Ca}|$ where $k_g$ and $h$ are extra-particle mass and heat transfer coefficients, respectively, $C_b$ and $T_b$ are steady state bulk concentration and temperature, respectively, and $\gamma = E_a/\mathrm{RT}_b$– were of the order of $10^{-4}$ ($\ll 0.05$), suggesting negligible transport effects.

## 3. Results and discussion

Figure 1 shows the effect of temperature on the NO oxidation reaction over $Pt/Al_2O_3$ in the temperature range 237–319 °C with 300 ppm NO, 0 or 170 ppm $NO_2$, 10% $O_2$, and a balance of $N_2$ as the gas flow. The rate is expressed as a turnover rate (TOR), defined as moles of NO reacted per second per mole of surface Pt. An apparent activation energy ($E_a$) of 82 kJ mol$^{-1}$ ± 9 KJ mol$^{-1}$ was obtained. A quantitative explanation for the difference in the $E_a$ between the experiments with and without $NO_2$ in the feed, as shown in the two curves in figure 1, will be given below in conjunction with equations (7) and (9). The deactivation in time (decrease in conversion with time under constant conditions) during the activation energy experiment was found to be about 16% at 300 °C. As detailed in Koryabkina *et al.* [11] the overall rate of this reversible reaction written in a power rate law form can be expressed as:

$$r = k_f[\mathrm{NO}]^a[\mathrm{O_2}]^b[\mathrm{NO_2}]^c(1-\beta) \qquad (1)$$

where $k_f$ is the forward rate constant, a, b and c are forward reaction orders and $\beta$ is the approach to equilibrium given as:

$$\beta = \frac{[\mathrm{NO_2}]}{K[\mathrm{NO}][\mathrm{O_2}]^{1/2}} \qquad (2)$$

with $K$ as the equilibrium constant. The values for $\beta$ in our experiments were in the range 0.02–0.14, which indicates that the reaction was carried out far from equilibrium. Note that the reversibility of the NO oxidation reaction is accounted for by using equation (1) above.

To determine the forward reaction orders, the concentrations were independently varied over the ranges: NO (100–450 ppm), $O_2$ (5–25%), and $NO_2$ (80–220 ppm). Figure 2 shows the effects of these concentrations on the NO oxidation turnover rate at 300 °C. The rate of NO consumption was close to first order with respect to both NO and $O_2$, while it was close to negative first order with respect to $NO_2$ over the concentration range studied. The catalyst deactivation over

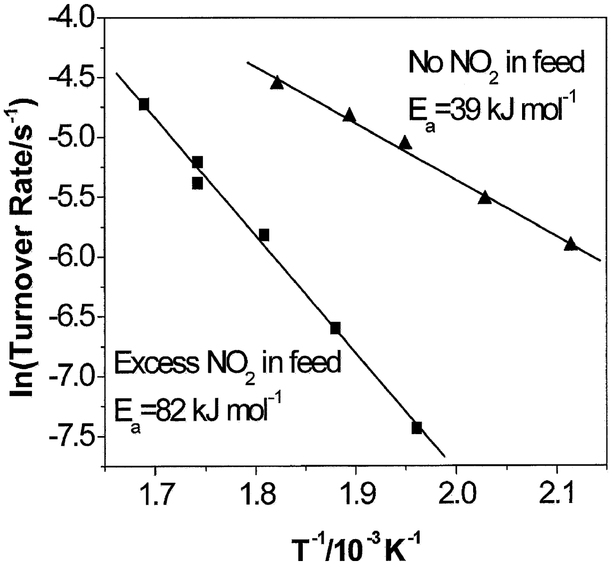

Figure 1. Arrhenius plot for NO oxidation on $Pt/Al_2O_3$ assuming a differential reactor. Feed: 300 ppm NO, 10% $O_2$, 0 or 170 ppm $NO_2$.

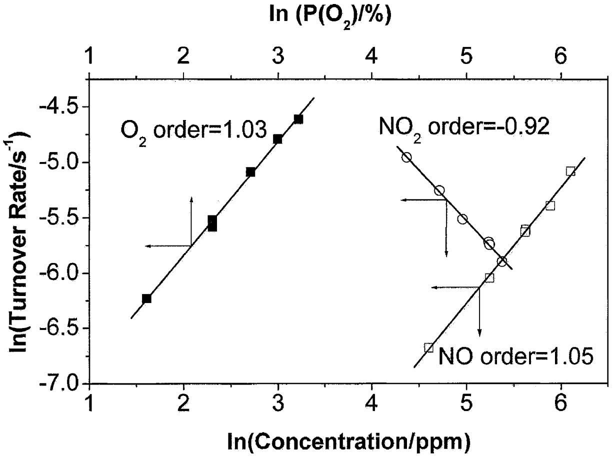

Figure 2. NO oxidation turnover rate (TOR) dependence on $O_2$, NO and $NO_2$ concentrations at 300 °C. Feed for NO order: 170 ppm $NO_2$, 10% $O_2$, 100–450 ppm NO; feed for $NO_2$ order: 10% $O_2$, 300 ppm NO, 80–220 ppm $NO_2$, feed for $O_2$ order: 300 ppm NO, 170 ppm $NO_2$, 5–25% $O_2$.

the full time of experiment was less than 2.5%. With the observed orders with respect to NO, $O_2$ and $NO_2$ as 1, 1 and −1, respectively, if there is no $NO_2$ in the feed, the forward reaction rate will be:

$$r = A\exp\left(\frac{-E_a}{RT}\right)\frac{[NO][O_2]}{[NO_2]}$$
$$= A\exp\left(\frac{-E_a}{RT}\right)\frac{(1-\chi)\{[O_2]_o - [NO]_o(\chi/2)\}}{\chi} \qquad (3)$$

where $\chi$ is the conversion of NO, $A$ is the pre-exponential factor, and $[C]_o$ represents the concentration of species C in the feed. With excess $O_2$ in the feed, as is the case for a lean-burn engine exhaust, and with low conversions such that $\chi$ is small with respect to 1 and$\{2[O_2]_o/[NO]_o\}$, the numerator of equation (3) becomes essentially independent of $\chi$, and then equation (3) simplifies to:

$$r = \frac{B\exp(-E_a/RT)}{\chi} \qquad (4)$$

where $B$ is $A[O_2]_o$. Note that the rate is still a function of conversion. Using this rate expression (4), the equation for a plug-flow reactor will then be:

$$\frac{d\chi}{d\tau} = \frac{B'\exp(-E_a/RT)}{\chi} \qquad (5)$$

where $B'$ is $B/[NO]_o$ and $\tau$ is the space time, the catalyst volume divided by the volumetric flow rate. The integration of equation (5) shows a linear relationship between the logarithm of conversion and inverse temperature with a slope of$-E_a/2R$ (equation (7)):

$$\chi^2 = 2B'\tau\exp(-E_a/RT) \qquad (6)$$

$$\ln\chi = \left(\frac{-E_a/2}{R}\right)\frac{1}{T} + \text{constant} \qquad (7)$$

On the other hand, with excess $NO_2$ and $O_2$ in the feed and the low NO conversions used in this study, the equation for a plug-flow reactor becomes:

$$\frac{d\chi}{d\tau} = A'\exp(-E_a/RT)\frac{[NO]_o(1-\chi)\{[O_2]_o - [NO]_o(\chi/2)\}}{[NO_2]_o + [NO]_o\chi} \qquad (8a)$$

$$= A''\exp(-E_a/RT) \qquad (8b)$$

where $A'$ is $A/[NO]_o$ and $A''$ is $A[O_2]_o/[NO_2]_o$. Equation (8b) is obtained from equation (8a) by neglecting $\chi$ ($\ll 1$) terms in comparison to other larger terms, thereby making the rate independent of conversion. The solution of equation (8b) is then:

$$\ln\chi = \left(\frac{-E_a}{R}\right)\frac{1}{T} + \text{constant} \qquad (9)$$

giving a linear relationship between the logarithm of conversion and inverse temperature with a slope of simply$-E_a/R$. In the differential conversion regime, the TOR is proportional to $\chi$ and ln(TOR) can replace $\ln(\chi)$ in equations (7) and (9). In a kinetic study of NO oxidation done in the absence of $NO_2$ in the feed [7], the apparent activation energy extracted from the data was ca. 40 kJ mol$^{-1}$, i.e., roughly half of the value reported here, in good agreement with the analysis above. Furthermore, when their data was corrected for $NO_2$ inhibition by integration of the reaction data an activation energy of 80 kJ mol$^{-1}$, close to our finding, was obtained. The apparent activation energy in the absence of excess $NO_2$ in the feed was also investigated in our lab and an apparent "activation energy" of 39 kJ mol$^{-1}$ ± 6 kJ mol$^{-1}$, again half of the value obtained with $NO_2$, was found, as shown in figure 1. Note that in both cases a model assuming no $NO_2$ inhibition (equation 4) was used. We take these results as confirmation of the $NO_2$ inhibition model.

Comparison of the values of the rates measured in this work with those in the literature is complicated since the literature studies were carried out under different conditions and the inhibitory effect of $NO_2$ was not fully considered. In the absence of $NO_2$ in the feed, the measured rate is a function of the conversion even at the lowest measurable values of conversion, and the apparent activation energy is lower if the reactor is assumed as differential. Also, it should be noted that the TOR for NO oxidation over Pt is known to be metal particle size dependent with larger Pt particles exhibiting higher activity than the smaller particles [1,8,12]. For our catalyst (0.296 wt% Pt per total weight, 42% PME), at 300 °C with 300 ppm NO, 170 ppm $NO_2$ and 10% $O_2$, the TOR calculated was $4.6 \times 10^{-3}$ s$^{-1}$. We also calculated the rate from the data reported by Lee and Kung [1] and Olsson *et al.* [7], correcting their values to our conditions, and found the TOR for a 0.27 wt% Pt/$Al_2O_3$ catalyst with 82% PME as $2.3 \times 10^{-3}$ s$^{-1}$ while for a 2.3 wt% Pt/$Al_2O_3$ catalyst with 4.5% PME, the TOR was 0.16 s$^{-1}$, under the same conditions listed above. Our TOR fits well into the observed trend of increasing rate with lower PME. With such dependence of TOR on particle size, the activation energy might also be expected to change with particle size. However, such an observation has not yet been reported in the literature.

The rate inhibition by $NO_2$ can be attributed to the fact that $NO_2$ adsorbs preferentially on the surface because of its high sticking coefficient on Pt [13,14], keeping it oxidized and preventing adsorption of other species. Thus, most of the surface oxygen, O*, which is taken to be the most abundant surface intermediate [7,15], comes from the dissociation of $NO_2$ [13] rather than from $O_2$ (step (11) in the scheme below). This is also suggested from Parker and Koel [14] and Segner *et al.* [13], who found that the high sticking coefficient of $NO_2$ makes it a very effective source of surface oxygen. Moreover, Zheng and Altman [16] found that on Pd (111), an oxygen coverage roughly an order of magnitude higher can be obtained with $NO_2$ exposures as compared to $O_2$. Based on the above information and our findings of the reaction orders, and using O* as the most abundant surface intermediate, we propose the following reaction steps to describe NO oxidation:

$$NO + * \overset{K_1}{\rightleftharpoons} NO* \tag{10}$$

$$NO_2 + 2* \overset{K_2}{\rightleftharpoons} NO * + O* \tag{11}$$

$$O_2 + * \xrightarrow{k_3} O_2* \tag{12}$$

$$O_2 * + * \xrightarrow{k_4} 2O* \tag{13}$$

where * denotes a Pt site and $K_i$ and $k_i$ the equilibrium constant and rate constant of the $i^{th}$ step. Assuming step (12) as the rate determining step (RDS), O* as the most abundant surface intermediate, and steps (10) and (11) in quasi-equilibrium, the rate expression obtained is:

$$r = \{k_3[L]\}\frac{[O_2]}{1 + \frac{K_2[NO_2]}{K_1[NO]}} \tag{14}$$

where $[L]$ denotes the total surface concentration of active metal sites. When the second term in the denominator is large compared to 1, implying that the coverage of O* is higher than the one for free sites *, equation (14) simplifies to:

$$r = \left\{\frac{k_3[L]K_1}{K_2}\right\}\frac{[NO][O_2]}{[NO_2]} \tag{15}$$

having the same concentration dependence as observed in our experiments. The overall rate constant of the NO oxidation reaction is thus given by$\{k_3[L]K_1/K_2\}$.

Other mechanisms have also been proposed in the literature [2,7,15,17]. For example, Olsson *et al.* [7] found $NO + O^* \rightarrow NO_2^*$ as the RDS based on their thermodynamic calculations, whereas we propose associative adsorption of $O_2$ as the RDS. Furthermore, the same authors could not confirm which mechanism (Langmuir-Hinshelwood, Eley-Rideal, or both) is most probable for NO oxidation as all of them seem to fit the experimental data equally well [15].

## 4. Conclusions

The effects of temperature, and reactant an product concentrations on the kinetics of NO oxidation on $Pt/Al_2O_3$ were investigated and a kinetic mechanism which fits the observed reaction orders is proposed. Under the conditions studied, the reaction had an activation energy of 82 ± 9 kJ $mol^{-1}$. The forward rate of $NO_2$ production was nearly first order with respect to both NO and $O_2$ concentrations and interestingly about negative first order with respect to $NO_2$ concentration. This inhibition effect was attributed to the strong oxidizing property of $NO_2$, which dissociatively adsorbs preferentially on Pt. This inhibition effect and the fact that generally a lean-burn exhaust mixture contains both NO and $NO_2$ [18] implies that $NO_2$ needs to be included in the kinetic tests and model development to capture the chemistry that occurs during reaction steps that involve NO oxidation.

## Acknowledgments

We thank the Indiana 21st Century Research and Technology Fund and Cummins, Inc. for financial support of this work. The authors would also like to acknowledge the Department of Energy (CRADA ORNL97-0489) for support. We are also grateful to Professor Gary E. Blau for so generously sharing his wisdom on modeling and statistical analysis of data.

## References

[1] J.-H.. Lee and H.H.. Kung, Catal. Lett. 51 (1998) 1.
[2] R. Burch and T.C. Watling, J. Catal. 169 (1997) 45.
[3] H. Ohtsuka, Appl. Catal. B 33 (2001) 325.
[4] W.S. Epling, L.E. Campbell, A. Yezerets, N.W. Currier and J.E. Parks, Catal. Rev. 46 (2004) 163.
[5] Control of Air Pollution from New Motor Vehicles: Heavy-Duty Engine and Vehicle Standards and Highway Diesel Fuel Sulfur Control Requirements. U.S. EPA, 80 and 86.
[6] A. Amberntsson, E. Fridell and M. Skoglundh, Appl. Catal. B 46 (2003) 429.
[7] L. Olsson, B. Westerberg, H. Persson, E. Fridell, M. Skoglundh and B. Andersson, J. Phys. Chem. B 103 (1999) 10433.
[8] E. Xue, K. Seshan and J.R.H. Ross, Appl. Catal. B 11 (1996) 65.
[9] J.E. Benson and M. Boudart, J. Catal. 4 (1965) 704.
[10] F.H.M. Dekker, A. Bliek, F. Kapteijn and J.A. Moulijn, Chem. Eng. Sci. 50 (1995) 3573.
[11] N.A. Koryabkina, A.A. Phatak, W.F. Ruettinger, R.J. Farrauto and F.H. Ribeiro, J. Catal. 217 (2003) 233.
[12] L. Olsson and E. Fridell, J. Catal. 210 (2002) 340.
[13] J. Segner, W. Vielhaber and G. Ertl, Isr. J. Chem. 22 (1982) 375.
[14] D.H. Parker and B. Koel, J. Vac. Sci. Technol. A 8 (1990) 2585.
[15] L. Olsson, H. Persson, E. Fridell, M. Skoglundh B. Andersson, J. Phys. Chem. B 105 (2001) 6895.
[16] G. Zheng and E.I. Altman, Surf. sci. 462 (2000) 151.
[17] E. Fridell, H. Persson, L. Olsson, B. Westerberg, A. Amberntsson and M. Skoglundh, Top Catal. 16/17 (2001) 133.
[18] S. Hodjati, K. Vaezzadeh, C. Petit, V. Pitchon and A. Kiennemann, Catal. Today 59 (2000) 323.